some specific types of surgeries.[12–14] However, of these three intraoperative parameters, the appropriate cutoff values for EBL may not be identical between surgeries because the amount of blood loss differs between different types of surgeries. Indeed, different cutoff values for EBL were proposed for patients undergoing total cystectomy, and this modified SAS (mSAS) proved to correlate with short-term morbidity and mortality.[14] However, the significance of the SAS and the appropriate cutoff values for EBL after gastrectomy, have not yet been evaluated.

Our aim in this study was to evaluate the predictability of the SAS for severe complications after gastrectomy. Furthermore, the predictability of an mSAS, in which the cutoff value for EBL was slightly adjusted, was evaluated.

METHODS

We investigated 328 patients who underwent gastrectomy with D1–2 lymph node dissection for primary gastric cancer at the Shizuoka Cancer Center in 2010. Clinicopathological data were collected from the database of our hospital. Intraoperative L-HR and L-MAP were collected from electronic medical records. This retrospective study was approved by the Human Ethics Review Committee of the Shizuoka Cancer Center.

The parameters evaluated in this study included intraoperative L-HR, L-MAP, and EBL. The original SAS (oSAS) was calculated by these three parameters (Table 1).[11] In addition, we developed an mSAS, in which the cutoff values for blood loss were set by the quartile values of the 328 patients in this study (Table 2). The median EBL was 274 mL (range 0–2,067 mL), and the interquartile range was 146–524 mL.

Other variables evaluated included age, sex, body mass index, preoperative albumin, type of surgery, thoracotomy, surgical approach, extent of lymph node dissection, operation time, tumor size, macroscopic type, cStage, and American Society of Anesthesiologists (ASA) score. The macroscopic type and cStage were determined according to the Japanese Gastric Cancer Association classification (3rd English edition).[15] We performed D2 lymph node dissection for patients with Stage IB or higher, while we performed D1+lymph node dissection for patients with Stage IA disease.

Evaluation of Complication Grade

We defined postoperative complications as any morbidities observed within 30 days after the first discharge. The severity of complication was graded using the Clavien–Dindo classification.[16] Patients with a Clavien–Dindo classification of grade IIIa or higher were defined as having severe complications.

Statistical Analysis

In this study, the Chi-square test was used for categorical variables, and the *t* test or Wilcoxon test was used for numerical variables, as appropriate.

Clinical characteristics and surgical findings were compared between patients with and without severe complications.

The receiver operating characteristic (ROC) analyses of the oSAS and mSAS were used to identify an appropriate cutoff level to predict severe complications.

All statistical analyses were performed with JMP software, version 8.0 (SAS Institute, Cary, NC, USA). p Values <0.05 were considered statistically significant, and all tests were two-sided.

RESULTS

Patient Characteristics

The mean age of the study population was 66.8 years, and about two-thirds of the patients were male (66.3 %). Approximately 60 % of patients were classified as Stage I. The most frequently performed operation was distal

TABLE 1 Evaluation of the original Surgical Apgar Score

	0 point	1 point	2 points	3 points	4 points
Estimated blood loss (mL)	>1,000	>600, ≤1,000	>100, ≤600	≤100	–
Lowest mean arterial pressure (mm Hg)	<40	≥40, <55	≥55, <70	≥70	–
Lowest heart rate (beats/min)	>85	>75, ≤85	>65, ≤75	>55, ≤65	≤55

TABLE 2 Cutoff values for estimated blood loss which were used in the modified Surgical Apgar Score

	0 point	1 point	2 points	3 points	4 points
Estimated blood loss (mL)	≥525	≥274, <525	≥147, <274	<147	–

gastrectomy (51.4 %), while total gastrectomy was performed in 97 patients (29.5 %). A D2 lymph node dissection was performed in 163 patients (49.7 %). Splenectomy was also performed in 47 patients (14.3 %).

Complications

There was no mortality within 30 days after the first discharge. Of the 328 patients included in our analysis, severe postoperative complications were observed in 36 patients (11.0 %). The most frequently observed severe complication was pancreatic fistula (n = 15; 4.6 %), followed by anastomotic leakage (n = 7; 2.1 %), pleural effusion (n = 6; 1.8 %), bowel obstruction (n = 5; 1.5 %), abdominal abscess (n = 3; 0.9 %), bleeding (n = 2; 0.6 %), pneumonia (n = 2; 0.6 %), and chylous ascites (n = 1; 0.3 %).

Distribution of Patients and Receiver Operating Characteristic (ROC) Analysis by Original Surgical Apgar Score (SAS)

The distribution of patients by the oSAS is shown in Fig. 1a. The area under the ROC curve for predicting severe complications by the oSAS was 0.65 (Fig. 2a). This analysis showed that the best cutoff line for the oSAS was

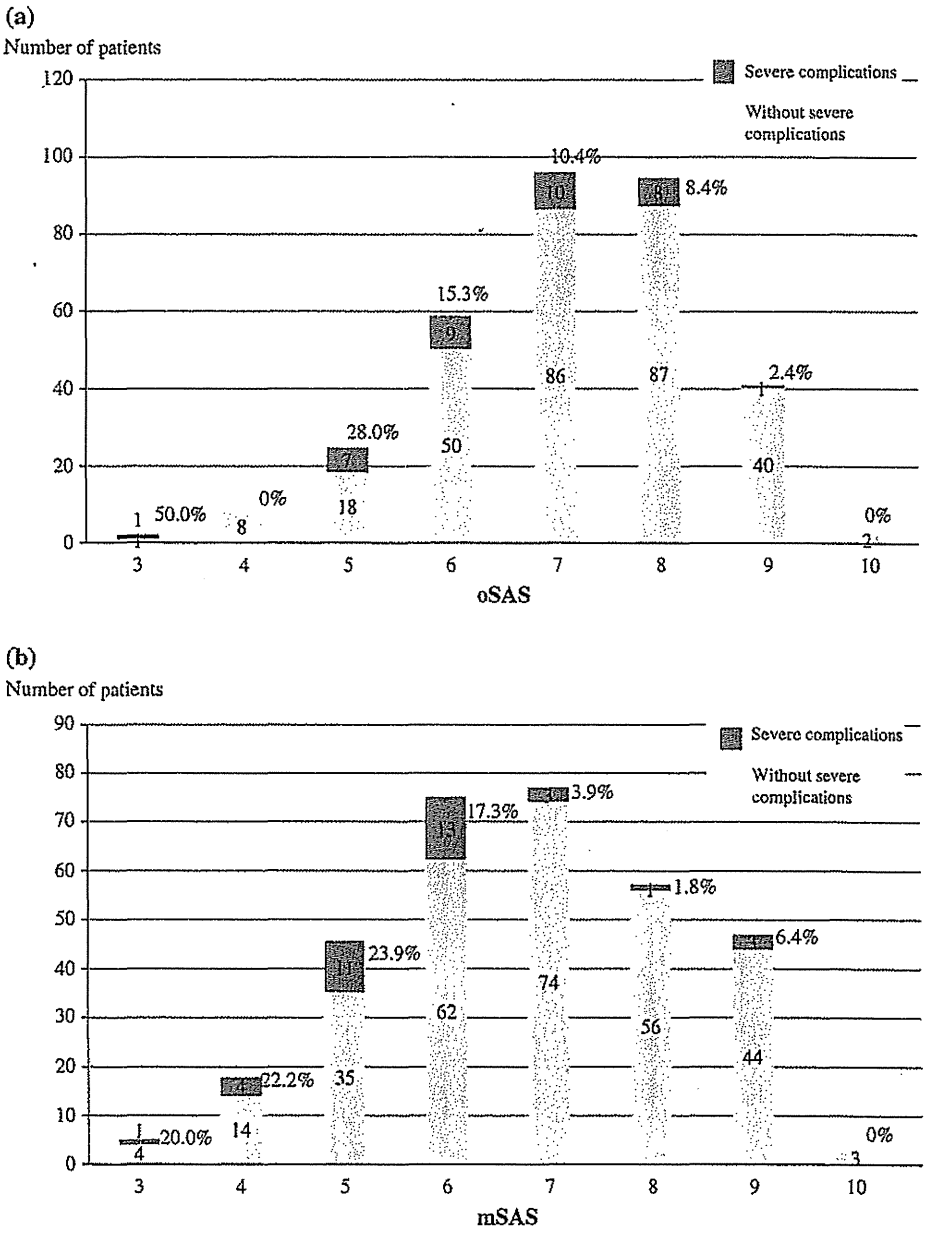

FIG. 1 Distribution of patients and proportion of severe complications by the (a) oSAS, and (b) mSAS. *oSAS* original Surgical Apgar Score, *mSAS* modified Surgical Apgar Score

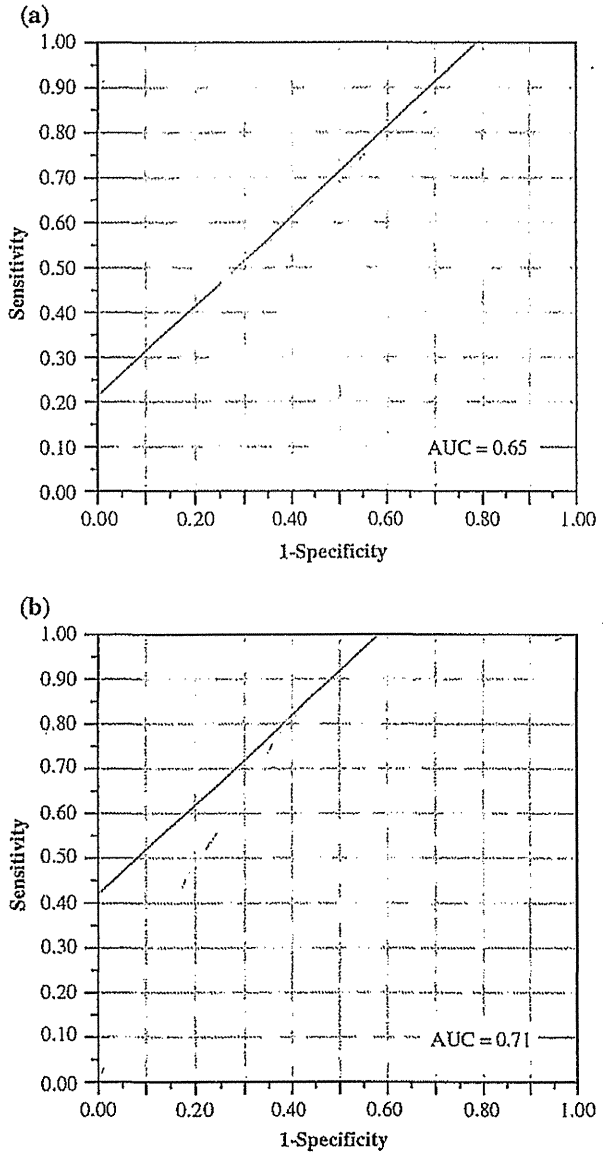

FIG. 2 Receiver operating characteristic curves for predicting severe complications by the (a) original SAS, and (b) modified SAS. *SAS* Surgical Apgar Score, *AUC* area under the curve

between six and seven points, at which sensitivity plus specificity was maximal. Sensitivity, specificity, and positive predictive value at each cutoff value for oSAS are shown in the electronic supplementary Table 1a. The number of patients under the cutoff value for the oSAS was 95 (28.9 %) (Fig. 1a).

Distribution of Patients and ROC Analysis by modified SAS

The distribution of patients by the mSAS is shown in Fig. 1b. The area under the ROC curve for predicting

TABLE 3 Association between patient characteristics and complication severity according to the Clavien–Dindo classification

Parameters	No. of patients (%) with complications		
	≤Grade II	≥Grade IIIa	*p* Value
Preoperative factors			
Sex			0.015
Male	187 (86.2)	30 (13.8)	
Female	105 (94.6)	6 (5.4)	
Age (years)			0.085
≥75	73 (83.9)	14 (16.1)	
<75	219 (90.9)	22 (9.1)	
Body mass index			0.850
≥25	69 (89.6)	8 (10.4)	
<25	223 (88.8)	28 (11.2)	
ASA score			0.506
0–1	97 (90.7)	10 (9.3)	
2–5	195 (88.2)	26 (11.8)	
Preoperative albumin (g/dL)			0.023
≥3.0	7 (63.6)	4 (36.4)	
<3.0	285 (89.9)	32 (10.1)	
Preoperative chemotherapy			0.083
Not performed	276 (89.9)	31 (10.1)	
Performed	16 (76.2)	5 (23.8)	
cStage			0.003
I, II	225 (92.2)	19 (7.8)	
III, IV	67 (79.8)	17 (20.2)	
Perioperative factors			
Operation			<0.001
Total gastrectomy	71 (73.2)	26 (26.8)	
Other	221 (95.7)	10 (4.3)	
Thoracotomy			0.016
Performed	3 (50.0)	3 (50.0)	
Not performed	289 (89.8)	33 (10.2)	
Surgical approach			0.023
Open	250 (87.7)	35 (12.3)	
Laparoscopic	42 (97.7)	1 (2.3)	
Lymph node dissection			0.021
D1, D1+	153 (92.7)	12 (7.3)	
D2	139 (85.3)	24 (14.7)	
Operation time (min)			<0.001
≥231	134 (81.3)	31 (18.7)	
<231	158 (96.9)	5 (3.1)	
oSAS			0.012
0–6	77 (82.0)	17 (18.0)	
7–10	215 (91.9)	19 (8.1)	
mSAS			<0.001
0–6	115 (79.9)	29 (20.1)	
7–10	177 (96.2)	7 (3.8)	

ASA American Society of Anesthesiologists, *oSAS*, original Surgical Apgar Score, *mSAS* modified Surgical Apgar Score

TABLE 4 Multivariate analysis of association between patient characteristics and postoperative complications rated as grade IIIa or higher by the Clavien–Dindo classification (oSAS selected as a covariate)

Variables	Odds ratio (95 % CI)	*p* Value
Sex (male)	2.07 (0.82–6.06)	0.128
Preoperative albumin (<3.0)	1.96 (0.40–9.09)	0.393
Preoperative chemotherapy (performed)	0.88 (0.24–2.90)	0.848
cStage (≥III)	0.98 (0.38–2.50)	0.976
Type of operation (TG)	5.96 (2.50–15.2)	<0.001
Extent of lymph node dissection (≥D2)	1.11 (0.45–2.75)	0.810
oSAS (≤6)	1.00 (0.42–2.34)	0.995
Operation time (≥231 min)	4.90 (1.80–15.9)	0.001

CI confidence interval, *TG* total gastrectomy, *oSAS* original Surgical Apgar Score

TABLE 5 Multivariate analysis of association between patient characteristics and postoperative complications rated as grade IIIa or higher by the Clavien–Dindo classification (mSAS selected as a covariate)

Variables	Odds ratio (95 % CI)	*p* Value
Sex (male)	2.14 (0.83–6.30)	0.115
Preoperative albumin (<3.0)	0.61 (0.14–2.94)	0.529
Preoperative chemotherapy (performed)	0.80 (0.22–2.61)	0.713
cStage (≥III)	0.95 (0.37–2.39)	0.922
Type of operation (TG)	5.25 (2.21–13.2)	<0.001
Extent of lymph node dissection (≥D2)	0.99 (0.40–2.50)	0.987
mSAS (≤6)	2.62 (1.01–7.46)	0.048
Operation time (≥231 min)	3.56 (1.26–11.8)	0.016

CI confidence interval, *TG* total gastrectomy, *mSAS* modified Surgical Apgar Score

severe complications by the mSAS was 0.71 (Fig. 2b). This analysis showed that the best cutoff line for the mSAS was between six and seven points. Sensitivity, specificity, and positive predictive value at each cutoff value for mSAS are shown in the electronic supplementary Table 1b. The number of patients under the cutoff value for the mSAS was 144 patients (43.9 %) (Fig. 1b).

Risk Factors for Severe Complications

Univariate analyses showed that the oSAS and mSAS, as well as sex, preoperative albumin, cStage, type of surgery, thoracotomy, surgical approach, operation time, and extent of lymph node dissection, were associated with severe complications (Table 3). Variables achieving a probability value <0.10 in a univariate analysis were included in a subsequent multivariate analysis to identify risk factors for severe complications. In the multivariate analysis, we did not include thoracotomy and surgical approach as covariates because these are apparent confounding factors for operative procedure; thoracotomy was used only for total gastrectomy, and laparoscopy was used only for distal gastrectomy in our institute. In the multivariate analysis, the type of surgery and operation time were selected as independent predictive factors for severe complications, while the oSAS was not (Table 4). On the other hand, when we included the mSAS as a covariate instead of the oSAS, the mSAS was selected as an independent predictive factor (Table 5).

DISCUSSION

In this study, we showed that the mSAS is a useful predictor for the development of severe complications after gastrectomy. With the mSAS, surgical teams can assess the risk of major complications immediately after surgery.

The SAS was first proposed by Gawande et al. in 2007.[11] Like the widely used obstetrical Apgar score developed by Virginia Apgar in 1953,[17] the SAS was intended for use immediately after surgery to predict patient outcomes. This surgical score reflects intraoperative hemodynamic stability, and is influenced by various factors such as the quality of surgery and anesthesia, and the patient's condition before and during surgery. At first, the SAS was validated in a cohort of patients who underwent colectomy and a cohort who underwent general and vascular surgery.[11,18,19] After that, modified versions of the SAS have been applied in other fields of surgery, including urology and neurosurgery.[12,14] However, the SAS has not yet been applied to patient cohorts who have undergone gastrectomy. To the best of our knowledge, the present study is the first to investigate the utility and significance of the SAS after gastrectomy for gastric cancer.

Several scoring models have been shown to effectively predict patient outcomes. However, they consist of many variables, which include subjective parameters, such as the severity of the patients' preoperative comorbidities, as indicated by the ASA score. The number of parameters required in the NSQIP, POSSUM, and E-PASS scores is 66, 18, and 9, respectively. Furthermore, all three scoring models need complex calculation formulae. On the contrary, the SAS uses only three intraoperative parameters, which are objective, and can be calculated easily. In addition, the area under the curve for the mSAS was not inferior to that of E-PASS or POSSUM when we calculated them with the same data set (data not shown).

Although EBL, L-MAP, and L-HR alone have been shown to be important predictors for complications in the past,[20,21] the combination of these three variables is a unique characteristic of the SAS.[11] We were able to notice intraoperative hemodynamic changes precisely using the three variables together, but not with a single variable. We

consider that intraoperative hypovolemia and hypoperfusion, reflected by an increased EBL, increased L-HR, and decreased L-MAP, lead to a lower perioperative tissue oxygenation, resulting in infectious complications.[22,23] In addition, lower L-MAP and higher L-HR might reflect intraoperative systemic inflammatory response syndrome, which has an increased postoperative complication rate.[24]

We set new cutoff values for EBL in this study. This kind of modification was also made in patients undergoing total cystectomy where a higher cutoff value for the oSAS was set because EBL during total cystectomy is usually higher than that during general surgeries. In our series, the median intraoperative blood loss was 274 mL which was thought to be lower than that in general surgery. Therefore, we adopted a new cutoff value for EBL; we used the quartile values of EBL in our mSAS. We consider appropriate cutoff values for EBL may be different depending on the type of surgery, although the cutoff values for L-MAP and L-HR should be the same in every type of surgery.

The present study showed that the mSAS is an independent risk factor for severe complications, while the oSAS is not. The oSAS was not selected as an independent risk factor even when we adopted a cutoff value other than ≤ 6 (data not shown). When we find patients with an mSAS ≤ 6, we should pay particular attention to the development of severe complications. For these patients, careful observation and intensive care are necessary.

Although the oSAS with slight modification is a useful scoring system to predict severe postoperative complications, this kind of modification reduces the universal appeal of the scoring system because different cutoff values have to be set when the SAS is used for different surgical procedures. From the point of view of general use, therefore, previously reported risk scoring models (POSSUM, E-PASS, etc.) may be superior to the SAS. Nevertheless, we still believe the mSAS is a promising scoring system because it is simple and as useful as POSSUM or E-PASS, and it can be calculated with ease at the bedside immediately after surgery. Accordingly, the SAS with slight modification can be applied easily in clinical practice if cutoff values are appropriately revised for specific types of surgery.

D2 lymphadenectomy has become a standard treatment for advanced gastric cancer in Western countries since the 15-year follow-up of the Dutch trial showed the survival benefit of D2 lymphadenectomy.[25] In Japan, although D2 lymphadenectomy has been a standard treatment for advanced gastric cancer, the Japanese guidelines allow less than a D2 lymphadenectomy for early gastric cancer. This is why we performed a D1 or D1+lymphadenectomy in 50.3 % of the patients in this study. However, Western randomized controlled trials have shown an increased incidence of intra-abdominal infection including pancreatic fistula after D2 lymphadenectomy compared with D1 lymphadenectomy, and Western guidelines recommend that D2 lymphadenectomies should only be performed at high-volume centers.[26,27] We believe the mSAS would be useful for the prediction of this potentially fatal complication.

The present retrospective study in a single institute has several limitations. First, the sample size was small to obtain any conclusive results. Second, it is unclear whether our cutoff value for EBL is also useful in Western countries. In Western countries, the average body mass index is higher than in Japan, resulting in longer operation times, higher EBL, and increased postoperative morbidity and mortality rates. Therefore, the appropriate cutoff value for EBL in Western countries may be different from that in the present study. We consider the cutoff value we set should be validated with a large number of patients, including Western patients, in the future. Third, although we believe that the appropriate cutoff value for EBL is different among different types of surgery, this concept has not been validated in surgeries other than total cystectomy. This issue should also be clarified in the future. Fourth, the SAS is not widely utilized in clinical practice, and it may be seen more as a research comparison tool. In addition, it is unclear whether appropriate control of the three variables improves patient outcome. Finally, about 60 % of patients had Stage I disease in our study, which is much higher than in Western countries. Accordingly, 50.3 % of patients underwent a D1+lymphadenectomy in our series. Therefore, for the results of the present study to be adopted in Western countries, a further validation study will be needed.

CONCLUSIONS

The oSAS was not found to be a significant predictive factor for severe complications after gastrectomy. On the contrary, our mSAS, in which the cutoff value for EBL was slightly modified, was considered to be a useful predictor for severe complications. The mSAS appears to be a useful tool for assessing the risk of severe complications immediately after surgery in patients with gastric cancer.

CONFLICTS OF INTEREST Yuichiro Miki, Masanori Tokunaga, Yutaka Tanizawa, Etsuro Bando, Taiichi Kawamura, and Masanori Terashima declare that they have no conflicts of interest.

REFERENCES

1. Sasako M. Principles of surgical treatment for curable gastric cancer. *J Clin Oncol.* 2003;21(23 Suppl):274-5s.
2. Koizumi W, Narahara H, Hara T, et al. S-1 plus cisplatin versus S-1 alone for first-line treatment of advanced gastric cancer (SPIRITS trial): a phase III trial. *Lancet Oncol.* 2008;9:215-21.

3. Kang YK, Kang WK, Shin DB, et al. Capecitabine/cisplatin versus 5-fluorouracil/cisplatin as first-line therapy in patients with advanced gastric cancer: a randomised phase III noninferiority trial. *Ann Oncol.* 2009;20:666-73.
4. Imamura H, Kurokawa Y, Kawada J, et al. Influence of bursectomy on operative morbidity and mortality after radical gastrectomy for gastric cancer: results of a randomized controlled trial. *World J Surg.* 2011;35:625-30.
5. Sano T, Sasako M, Yamamoto S, et al. Gastric cancer surgery: morbidity and mortality results from a prospective randomized controlled trial comparing D2 and extended para-aortic lymphadenectomy. Japan Clinical Oncology Group study 9501. *J Clin Oncol.* 2004;22:2767-73.
6. Sasako M, Sano T, Yamamoto S, et al. Left thoracoabdominal approach versus abdominal-transhiatal approach for gastric cancer of the cardia or subcardia: a randomised controlled trial. *Lancet Oncol.* 2006;7:644-51.
7. Copeland GP, Jones D, Walters M. POSSUM: a scoring system for surgical audit. *Br J Surg.* 1991;78:355-60.
8. Fink AS, Campbell DA Jr, Mentzer RM Jr, et al. The National Surgical Quality Improvement Program in non-veterans administration hospitals: initial demonstration of feasibility. *Ann Surg.* 2002;236:344-53;discussion 353-4.
9. Khuri SF, Daley J, Henderson W, et al. The Department of Veterans Affairs' NSQIP: the first national, validated, outcome-based, risk-adjusted, and peer-controlled program for the measurement and enhancement of the quality of surgical care. National VA Surgical Quality Improvement Program. *Ann Surg.* 1998;228:491-507.
10. Haga Y, Ikei S, Ogawa M. Estimation of Physiologic Ability and Surgical Stress (E-PASS) as a new prediction scoring system for postoperative morbidity and mortality following elective gastrointestinal surgery. *Surg Today.* 1999;29:219-25.
11. Gawande AA, Kwaan MR, Regenbogen SE, Lipsitz SA, Zinner MJ. An Apgar score for surgery. *J Am Coll Surg.* 2007;204:201-8.
12. Ziewacz JE, Davis MC, Lau D, El-Sayed AM, Regenbogen SE, Sullivan SE, et al. Validation of the surgical Apgar score in a neurosurgical patient population. *J Neurosurg.* 2013;118:270-9.
13. Thorn CC, Chan M, Sinha N, Harrison RA. Utility of the Surgical Apgar Score in a district general hospital. *World J Surg.* 2012;36:1066-1073.
14. Prasad SM, Ferreria M, Berry AM, et al. Surgical apgar outcome score: perioperative risk assessment for radical cystectomy. *J Urol.* 2009;181:1046-52;discussion 1052-3.
15. Japanese Gastric Cancer Association. Japanese classification of gastric carcinoma: 3rd English edition. *Gastric Cancer.* 2011;14:101-12.
16. Clavien PA, Barkun J, de Oliveira ML, et al. The Clavien-Dindo classification of surgical complications: five-year experience. *Ann Surg.* 2009;250:187-96.
17. Apgar V. A proposal for a new method of evaluation of the newborn infant. *Curr Res Anesth Analg.* 1953;32:260-7.
18. Regenbogen SE, Bordeianou L, Hutter MM, Gawande AA. The intraoperative Surgical Apgar Score predicts postdischarge complications after colon and rectal resection. *Surgery.* 2010;148:559-66.
19. Regenbogen SE, Lancaster RT, Lipsitz SR, Greenberg CC, Hutter MM, Gawande AA. Does the Surgical Apgar Score measure intraoperative performance? *Ann Surg.* 2008;248:320-8.
20. Reich DL, Bennett-Guerrero E, Bodian CA, Hossain S, Winfree W, Krol M. Intraoperative tachycardia and hypertension are independently associated with adverse outcome in noncardiac surgery of long duration. *Anesth Analg.* 2002;95:273-7.
21. Wolters U, Wolf T, Stutzer H, Schroder T. ASA classification and perioperative variables as predictors of postoperative outcome. *Br J Anaesth.* 1996;77:217-22.
22. Ives CL, Harrison DK, Stansby GS. Tissue oxygen saturation, measured by near-infrared spectroscopy, and its relationship to surgical-site infections. *Br J Surg.* 2007;94:87-91.
23. Meyhoff CS, Wetterslev J, Jorgensen LN, et al. Effect of high perioperative oxygen fraction on surgical site infection and pulmonary complications after abdominal surgery: the PROXI randomized clinical trial. *JAMA* 2009;302:1543-50.
24. Kelly KJ, Greenblatt DY, Wan Y, Rettammel RJ, Winslow E, Cho CS, et al. Risk stratification for distal pancreatectomy utilizing ACS-NSQIP: preoperative factors predict morbidity and mortality. *J Gastrointest Surg.* 2011;15:250-9;discussion 259.
25. Songun I, Putter H, Kranenbarg EM, Sasako M, van de Velde CJ. Surgical treatment of gastric cancer: 15-year follow-up results of the randomised nationwide Dutch D1D2 trial. *Lancet Oncol.* 2010;11:439-49.
26. Bonenkamp JJ, Songun I, Hermans J, et al. Randomised comparison of morbidity after D1 and D2 dissection for gastric cancer in 996 Dutch patients. *Lancet.* 1995;345:745-8.
27. Waddell T, Verheij M, Allum W, Cunningham D, Cervantes A, Arnold D. Gastric cancer: ESMO-ESSO-ESTRO Clinical Practice Guidelines for diagnosis, treatment and follow-up. *Ann Oncol.* 2013;24 Suppl 6:vi57-63.

Gastric Cancer
DOI 10.1007/s10120-014-0426-3

ORIGINAL ARTICLE

A novel splice variant of XIAP-associated factor 1 (XAF1) is expressed in peripheral blood containing gastric cancer-derived circulating tumor cells

Keiichi Hatakeyama · Yushi Yamakawa · Yorikane Fukuda · Keiichi Ohshima · Kanako Wakabayashi-Nakao · Naoki Sakura · Yutaka Tanizawa · Yusuke Kinugasa · Ken Yamaguchi · Masanori Terashima · Tohru Mochizuki

Received: 12 April 2014 / Accepted: 23 August 2014

Abstract
Background XIAP-associated factor 1 (XAF1) is ubiquitously expressed in normal tissues, but its suppression in cancer cells is strongly associated with tumor progression. Although downregulation of XAF1 is observed in tumors, its expression profile in the peripheral blood of cancer patients has not yet been investigated. Here, we identified a novel *XAF1* splice variant in cancer cells and then investigated the expression level of this variant in peripheral blood containing gastric cancer-derived circulating tumor cells (CTCs).

Methods To identify splice variants, RT-PCR and DNA sequencing were performed in mRNAs extracted from many cancer cells. We then carried out quantitative RT-PCR to investigate expression in peripheral blood from all 96 gastric cancer patients and 22 healthy volunteers.
Results The XAF1 variant harbored a premature termination codon (PTC) and was differentially expressed in highly metastatic cancer cells versus the parental cells, and that nonsense-mediated mRNA decay (NMD) was suppressed in the variant-expressing cells. Furthermore, splice variants of *XAF1* were upregulated in peripheral blood containing CTCs. In *XAF1* variant-expressing patients, the expression levels of other NMD-targeted genes also increased, suggesting that the NMD pathway was suppressed in CTCs.
Conclusions Our study identified a novel splice variant of *XAF1* in cancer cells. This variant was regulated through the NMD pathway and accumulated in NMD-suppressed metastatic cancer cells and peripheral blood containing CTCs. The presence of XAF1 transcripts harboring the PTC in the peripheral blood may be useful as an indicator of NMD inhibition in CTCs.

Keywords Alternative splicing · Circulating tumor cells · Gastric cancer · Nonsense-mediated mRNA decay · Quantitative real-time polymerase chain reaction (qRT-PCR)

K. Hatakeyama and Y. Yamakawa equally contributed to this work.

Electronic supplementary material The online version of this article (doi:10.1007/s10120-014-0426-3) contains supplementary material, which is available to authorized users.

K. Hatakeyama · Y. Fukuda · K. Ohshima · K. Wakabayashi-Nakao · N. Sakura · T. Mochizuki
Medical Genetics Division, Shizuoka Cancer Center Research Institute, Shizuoka, Japan

Y. Yamakawa · Y. Tanizawa · M. Terashima (✉)
Division of Gastric Surgery, Shizuoka Cancer Center Hospital, 1077 Shimonagakubo, Nagaizumi-cho, Sunto-gun, Shizuoka 411-8777, Japan
e-mail: m.terashima@scchr.jp

Y. Yamakawa · Y. Kinugasa
Division of Colon and Rectal Surgery, Shizuoka Cancer Center Hospital, Shizuoka, Japan

Present Address:
Y. Fukuda
G&G Science, Fukushima, Japan

K. Yamaguchi
Shizuoka Cancer Center Hospital and Research Institute, Shizuoka, Japan

Introduction

XIAP-associated factor 1 (XAF1) has been identified as a nuclear protein and a binding partner that directly interacts with endogenous X-linked inhibitor of apoptosis (XIAP) [1]. XAF1 overexpression induces apoptosis and inhibits

Published online: 13 September 2014

tumor growth in multiple types of cancer including gastric, colorectal, and pancreatic cancers [2–7]. *XAF1* is ubiquitously expressed in normal cells but expressed at extremely low levels in several types of cancer cells [8]. Lower expression of this gene in tumor tissues is strongly associated with tumor stage [2, 5, 9, 10]. Splice variants of *XAF1* have been detected in various cancer cell lines [11–13]. Fang et al. [14] found a switch from full-length to short XAF1 transcripts in prostate cancer cells, suggesting differential function of the short variant in apoptosis regulation. The production of these transcripts is regulated through aberrant epigenetic modification [12–14]. However, the expression profile of *XAF1* splice variants in human cancer remains unclear.

Nonsense-mediated RNA decay (NMD) helps the cell to maintain mRNA quality [15]. Abnormal transcripts generated by alternative splicing often harbor premature termination codons (PTC), leading to degradation of these transcripts via the NMD pathway. NMD is suppressed by cellular stresses in the tumor microenvironment, the inhibition of which promotes stabilization of NMD-targeted mRNA and tumorigenesis [16–19]. Recently, Tani et al. [20] reported that accumulation of noncoding RNA growth-arrest-specific 5 (GAS5) by NMD inhibition through cellular stress (such as serum starvation) leads to the downregulation of apoptosis-related genes. Thus, aberrant RNAs that accumulate through NMD inhibition are considered to be potential tumor markers or biomarkers.

Although a meta-analysis of the published literature revealed that circulating tumor cells (CTCs) are involved in the poor prognosis of gastric cancer patients [21], the associated gene expression profiles remain unclear. Epithelial-mesenchymal transition (EMT)-related genes have been shown to be often expressed in CTCs [22–24], and several genes are abnormally spliced in the EMT [25–27]. RNA-Seq analysis revealed that alternative splicing can induce critical aspects of EMT-associated phenotypic changes, suggesting that the EMT is closely related to RNA splicing [28]. Recently, Valacca et al. [29] reported that aberrantly spliced transcripts accumulated as a result of NMD inhibition in an in vitro model of the EMT. Thus, CTCs in which the EMT is occurring may demonstrate alternative splicing that generates transcripts which would normally be targeted by NMD.

Quantitative real-time polymerase chain reaction (qRT-PCR) is one of the most sensitive methods for evaluation of gene expression and is utilized to detect mRNA tumor markers in peripheral blood, such as mRNA encoding cytokeratin 19 (*CK19*), cytokeratin 20 (*CK20*), and carcinoembryonic antigen (CEA; synonym, *CEACAM5*) [30–32]. The PAXgene qRT-PCR assay can detect stabilized RNA in the peripheral blood, thus reflecting the expression level of transcripts in CTCs, which showed strong concordance with the results of CTC counting by immunomagnetic separation (CellSearch; Janssen Diagnostics, Raritan, NJ, USA) [33, 34]. However, several markers detected in peripheral blood are frequently expressed in normal epithelial cells, resulting in decreased sensitivity and specificity of qRT-PCR [35]. To maintain the performance of this method using peripheral blood samples, cancer-specific transcripts must be selected [34, 36].

In this study, to evaluate the potential utility of a splice variant harboring PTC as a biomarker or tumor marker, we investigated the presence of aberrant *XAF1* transcripts in cancer cell lines and in the peripheral blood of patients with gastric cancer using qRT-PCR. The RT-PCR analysis and DNA sequencing revealed that a novel splice variant of *XAF1* was expressed in gastric, pancreatic, colorectal, and breast cancer cell lines. This splice variant harboring PTC accumulated in NMD-suppressed cells. Furthermore, the *XAF1* variant in peripheral blood containing CTCs obtained from patients with gastric cancer was significantly upregulated relative to samples from healthy volunteers. These findings suggest that the novel *XAF1* variant identified in this study is a potential blood biomarker.

Materials and methods

Patients and specimens

From April 2010 to August 2012, PAXgene (PreAnalytiX; Hombrechtikon, Switzerland) was used to collect peripheral blood samples (2.5 ml) from 96 patients [65 men, 31 women; median age, 67 (30–85) years] with gastric cancer at Shizuoka Cancer Center Hospital and from 22 healthy volunteers [16 men, 6 women; median age, 36 (26–70) years] who were coworkers at the hospital. Informed consent was obtained from all patients, and the Institutional Review Board at Shizuoka Cancer Center approved all aspects of this study.

Cell cultures, RNA sample preparation, and RT-PCR

The cell lines used in this study are listed in Table S1 in the Supplementary Material. cDNA for different splice variants of *XAF1* was screened using the intron-spanning exonic primers listed in Table S2 in the Supplementary Material. The methods are described in detail in the Supplementary Material.

DNA sequencing analysis

To determine the sequence of the novel *XAF1* transcript, rapid amplification of cDNA ends (RACE) was conducted

using the GeneRacer Kit (Life Technologies, Carlsbad, CA, USA) according to the manufacturer's instructions. The primer sequences are shown in Table S2. The methods used for DNA sequencing analysis are provided in detail in the Supplementary Material.

Quantitative real-time PCR

Quantitative real-time PCR (qRT-PCR) was performed using the SYBR Green dye technique and the ABI PRISM 7900HT Fast Real-Time PCR System (Life Technologies). The methods and the validation results are described in detail in the Supplementary Material.

NMD inhibition assay with caffeine

The method for inhibiting NMD was previously described in detail [37]. Briefly, cells were seeded in two culture plates, and caffeine (10 mM) was added to one plate. Following 4 h of incubation, the medium was removed from both plates and the cells were washed twice with phosphate-buffered saline. Both actinomycin D (actD, 2 mg/ml) and caffeine (10 mM) were added to one plate (pretreated with caffeine), and actD alone was added to the other plate. After a further 4 h incubation, total RNA was obtained from both plates (see details in the Supplementary Material).

Statistical analysis

The coefficient of determination in the qRT-PCR standard curve was derived by Pearson's correlation analysis. *XAF1* and survivin (Baculoviral IAP Repeat Containing 5, *BIRC5*) expression levels in gastric cancer patients and healthy volunteers were depicted as box plots containing outliers and extreme outliers. The inner and outer fences for the plotting of the outliers were calculated using the 1.5× interquartile range (IQR) and 3.0× IQR, respectively. Because of the difference in sample size between patients and volunteers, the p value of the qRT-PCR analysis was calculated based on Welch's t test. Receiver operating characteristic (ROC) curves were computed using the R software and the associated pROC package [38]. The area under the curve (AUC) and optimal threshold (cutoff value), i.e., the point closest to the top left in the plot, were calculated in R. The 95 % confidence interval (CI) was computed to assess the variability of the measure using 10,000 bootstrap replicates [39]. Gene expression and clinicopathological characteristics according to the Japanese Classification of Gastric Carcinoma, 14th edition, were compared using Fisher's exact test. Significance was defined as $p < 0.05$.

Results

Identification of novel *XAF1* exons

Several splice variants of *XAF1* are known to be expressed in cancer cell lines [11–14]. To analyze the variants, we initially characterized the expression pattern of *XAF1* in the highly metastatic gastric cancer cell MKN45P (Fig. 1a). RT-PCR was conducted using previously reported primers [12] and newly designed primers to detect known transcripts and novel variants, respectively. Electrophoresis of the RT-PCR amplicons revealed that an unknown transcript candidate (*XAF1F*) was coexpressed with *XAF1A* and *XAF1C* in MKN45P. PCR-based cloning and DNA sequencing analysis using RACE subsequently showed that *XAF1F* was a novel splice variant (Fig. 1b). Specifically, this variant lacked exon 5 and possessed a unique exon 3 that contained exon 3-ext derived from the intronic region, resulting in seven exons. The sequence of the novel exonic region had a stop codon that was regarded as a PTC.

XAF1F expression in cancer cell lines

XAF1 transcripts are downregulated or absent in colorectal cancer cells [12]. We thus investigated the expression profile of *XAF1F* transcripts in gastrointestinal (colorectal, gastric, and pancreatic) and breast cancer cell lines using RT-PCR analysis (Fig. 2). The *XAF1F* transcript was expressed in 20 cell lines (20/45, 44 %) and also coexisted with other XAF1 transcripts (*XAF1A/C*) in 20 cell lines (20/20, 100 %). However, 10 of 32 *XAF1A*-expressing cell lines did not express the XAF1F transcript (10/32, 31 %). These results suggest that although *XAF1F* harboring PTC was often degraded by the NMD pathway, this transcript was coexpressed with other *XAF1*s in many cancer cells.

mRNA expression of NMD-related genes

Although *XAF1F* possessed a PTC in its mature mRNA sequence, it was expressed in 20 cancer cell lines. Among them, comparison of two pairs of cell lines (MKN45P vs. MKN45 and KP-3L vs. KP-3) in a metastatic model obtained by xenografting (for details, see Table S1) revealed that XAF1 expression, including that of *XAF1F*, in highly metastatic cells was higher than that in the parental cells (Fig. 2 and S2 in the Supplementary Material). To investigate NMD activity in variant-expressing cells, qRT-PCR for NMD-related genes was performed using these pairs (Fig. 3a). In MKN45P cells, the NMD target transcripts *ATF3* [16, 40] and *MAFF*

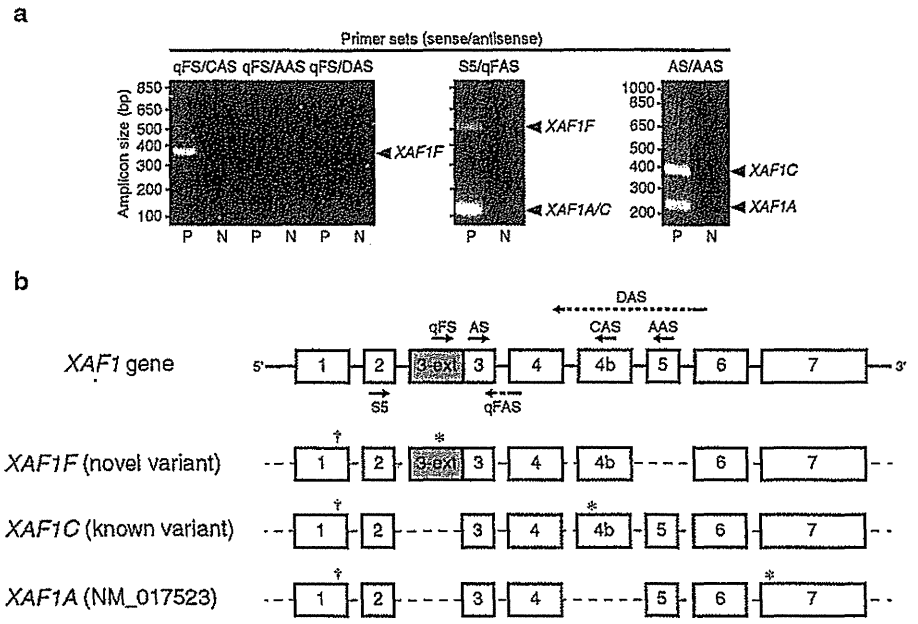

Fig. 1 Identification of a novel XIAP-associated factor 1 (*XAF1*) transcript. **a** Detection of *XAF1* transcripts expressed in a gastric cancer cell line (MKN45P). The novel transcript (*XAF1F*) was detected by RT-PCR using the primer sets qFS/CAS and S5/qFAS (sense/antisense). *P* and *N* under the *individual lanes* indicate the positive control (RT-PCR with MKN45P template) and negative control (without template), respectively. **b** Schematic representation of the exon structures of the *XAF1* gene and transcripts identified in this study. The *gray boxes* show a novel exonic region extending from known exon 3 in the *XAF1* gene, resulting in 8 exons. The primer positions for RT-PCR are indicated by *arrows*. Primers qFAS and DAS are designed to step over the intron between exons 3 and 4 and exons 4b and 5, respectively. The *dagger* and *asterisk* symbols indicate the locations of the start and stop codon, respectively

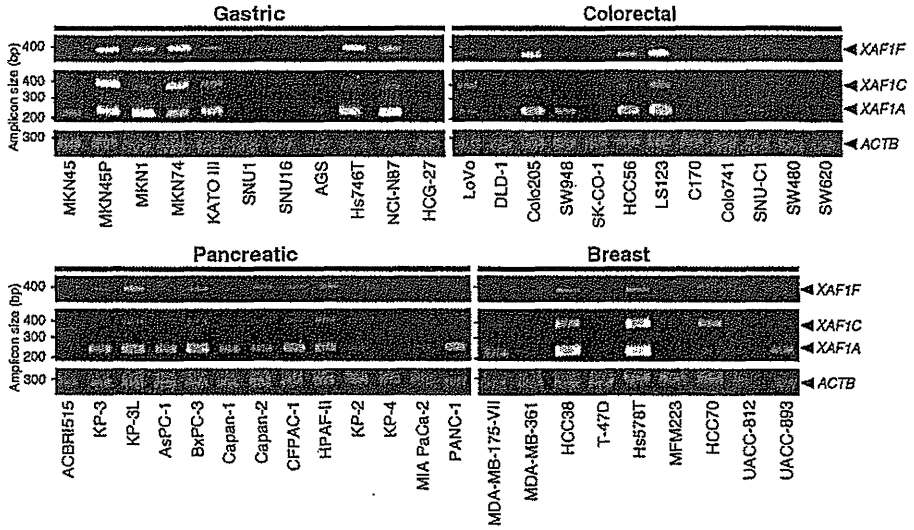

Fig. 2 Expression profile of *XAF1* transcripts in gastric, colorectal, pancreatic, and breast cancer cell lines. The transcripts of *XAF1F* and *XAF1A/C* were detected by RT-PCR using specific primer sets qFS/CAS and AS/AAS (sense/antisense), respectively. RT-PCR for beta-actin (*ACTB*) was conducted as a positive control experiment. Agarose gels were used at a concentration of 2 %

[41] were upregulated but the NMD factor *UPF1* [16, 41] was downregulated, indicating that the NMD pathway was inhibited. In KP-3L cells, mRNA expression of *ATF3*, *GADD45B* [16], and *UPF1* was significantly increased.

XAF1 expression in NMD-inhibited cells

To determine whether the transcript was degraded through the NMD pathway, we performed an NMD inhibition assay using caffeine and actD (Fig. 3b). The combination of

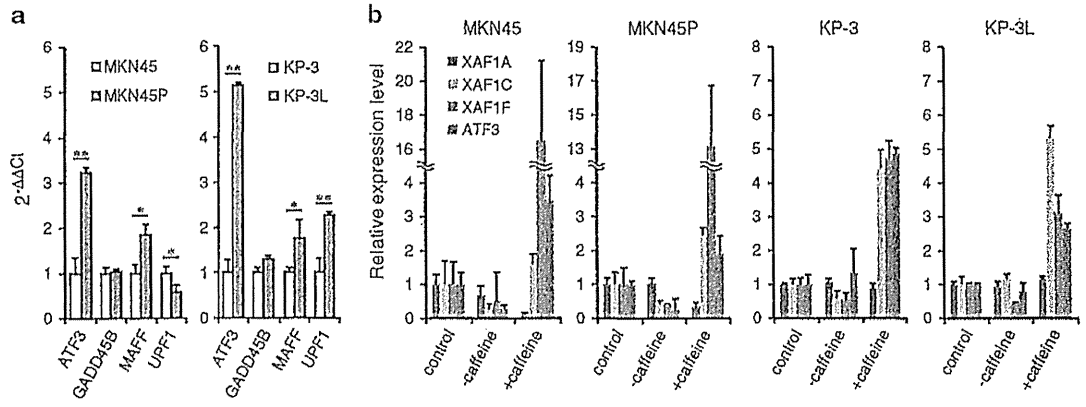

Fig. 3 Expression analysis of nonsense-mediated mRNA decay (NMD)-related and *XAF1* transcripts in pairs of cell lines used as a metastatic model. a Comparison of NMD-related gene expression between highly metastatic cells and their parental cells. The pairs of gastric cells (MKN45 vs. MKN45P) and pancreatic cells (KP-3 vs. KP-3L) are shown in *left* and *right panels*, respectively. The expression levels in the parental cells (MKN45 or KP-3) are shown as 1.0. SD was calculated from the relative expression level of triplicates. Statistical significance ($*p < 0.05$ and $**p < 0.01$) was evaluated by Student's *t* test. b Expression levels of *XAF1* transcripts in NMD-inhibited cancer cells. NMD was inhibited by caffeine and actD treatment (+caffeine). Treatment with actD alone (−caffeine) was used to observe RNA stability after blockade of transcription. Cancer cells that were not treated with reagents are presented as the control. The expression levels of *XAF1A* and *XAF1C* were estimated based on previous reports [12]. qRT-PCR of *ATF3* was conducted to determine NMD inhibition

these reagents was adopted to block increased transcription resulting from a stress response to NMD inhibition [37]. The NMD target transcript *ATF3* was upregulated in caffeine-treated cancer cells, indicating that the NMD pathway was inhibited by this treatment. Furthermore, mRNA expression of *XAF1C* and *XAF1F* harboring PTC was significantly increased in NMD-inhibited cancer cells. These upregulations were observed in other colorectal and breast cancer cells expressing *XAF1F* (Fig. S3 in the Supplementary Material).

Quantification of *XAF1F* in the peripheral blood of gastric cancer patients

Peripheral blood samples from all 96 patients and the 22 healthy volunteers were collected using PAXgene to stabilize whole RNA in the blood and subsequently evaluated using our qRT-PCR assay and semiquantitative RT-PCR as previously reported [12] (Fig. 4). To minimize the influence of RNA degradation on PCR, the RNA from all the samples was confirmed to have an RNA integrity number (RIN) [42] of at least 6.5 [43] (data not shown). *XAF1F* and *XAF1C* expression levels were significantly increased in patients relative to healthy volunteers. To investigate the relationship between age and mRNA expression, we calculated Spearman's rank correlation coefficient (ρ) for the samples (Table S3 in the Supplementary Material). The ρ value in the targeted genes was low, indicating a very weak to negligible correlation, suggesting that the expression was independent of age. These results indicate that *XAF1* splice variants were upregulated in the peripheral blood of gastric cancer patients.

mRNA expression of NMD-related genes in peripheral blood containing CTCs

qRT-PCR performed using peripheral blood collected with PAXgene can detect transcripts in CTCs [33, 34]. Recently, several research groups reported that CTC-derived survivin (*BIRC5*) was frequently detected in the peripheral blood of gastrointestinal cancer patients and that the mRNA expression level of this gene is useful as a prognostic factor [36, 44–47]. Therefore, to isolate CTC-positive samples, we adopted the *BIRC5* gene as a marker and performed a qRT-PCR assay for the quantification of *BIRC5* and *XAF1F* transcripts (Fig. S4 in the Supplementary Material). The prediction performance for CTC detection was evaluated using a ROC curve (Fig. 5). The AUC and cutoff values were 0.8299 (95 % CI, 0.7311–0.9048) and 180.75 (sensitivity, 82.99 %; specificity, 77.27 %), respectively. These data indicate that *BIRC5* expression, as measured by our qRT-PCR assay, is an efficient predictor for CTCs in the peripheral blood of gastric cancer patients. Using the calculated cutoff value, 79 CTC-positive samples were identified from 96 patients with gastric cancer.

To investigate the relationship between *XAF1* splice variants and the NMD target gene *ATF3* in the CTC-positive population, we also performed a ROC curve analysis for *XAF1F* and *XAF1C* (Fig. S5 in the Supplementary Material). Although the AUC of the variants was lower

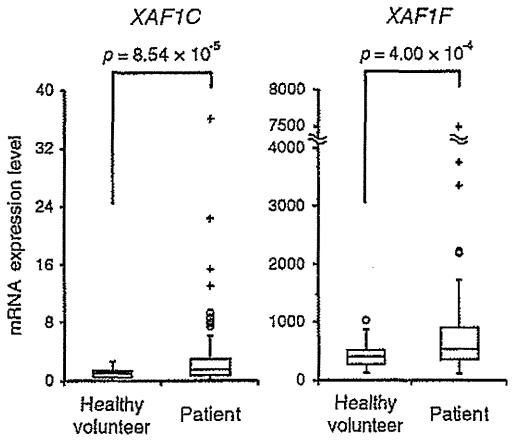

Fig. 4 Quantification of *XAF1F* and *XAF1C* transcripts in peripheral blood. *XAF1F* and *XAF1C* expression in gastric cancer patients ($n = 96$) and healthy volunteers ($n = 22$) was quantified using the qRT-PCR assay described in Figure S1 in the Supplementary Material. The normal and extreme outliers are indicated by *circle* and *plus symbols*, respectively

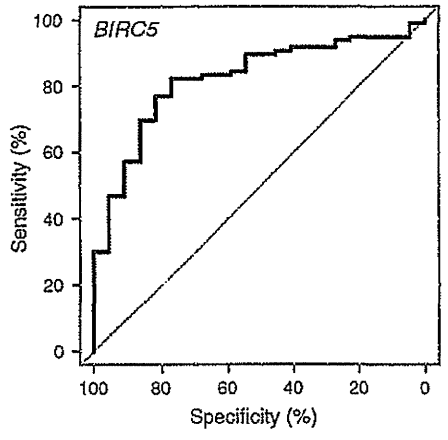

Fig. 5 ROC curve of *BIRC5* expression in peripheral blood. The *black solid line* indicates the curve for *BIRC5* in all peripheral blood samples ($n = 118$)

than that of *BIRC5*, the cutoff values were determined from the ROC curve. Table 1 shows *ATF3* expression in *XAF1C/F*-positive and *XAF1C/F*-negative populations distinguished by these values. The *XAF1F*- and *XAF1C*-positive patients accounted for 62.0 % (49/79) and 45.6 % (36/79), respectively, of the patients with CTCs. The population that was positive for both variants expressed the *ATF3* transcript. The expression level of *ATF3* in the positive patients was higher than that in the negative patients.

To further evaluate the differences in the patients with CTCs in the *XAF1C/F*-positive and *XAF1C/F*-negative populations, we correlated clinicopathological characteristics with the expression level of the splice variants

Table 1 mRNA expression level of *XAF1* variants and *ATF3* in gastric cancer patients

	Sample number	*ATF3*	
		Expression level (mean ± SD)	*p* value
In all patients			
BIRC5+	79	1.06 ± 0.51	NS
BIRC5−	17	0.87 ± 0.47	
In *BIRC5*-positive patients			
XAF1F+	49	1.15 ± 0.54	0.032
XAF1F−	30	0.92 ± 0.42	
XAF1C+	36	1.27 ± 0.61	0.0013
XAF1C−	43	0.89 ± 0.31	
XAF1F/C+	26	1.33 ± 0.62	0.0040
XAF1F/C−	53	0.93 ± 0.38	

Test used: Welch's *t* test

NS not significant

(Table 2). Among tumors invading into the subserosa (SS) or further, 74 % (29/39) expressed the *XAF1F* transcript, whereas 50 % (20/40) of tumors invading the muscularis propria (MP) were *XAF1F* negative ($p = 0.0368$). Comparison of patients with *XAF1F* expression demonstrated that 59 % (29/49) of the tumors in those patients invaded as far as the SS or further. Among patients with venous invasion, 80 % (32/40) were *XAF1F* positive, whereas 56 % (22/39) of patients without venous invasion did not show expression of *XAF1F* ($p = 0.0011$). In the *XAF1F*-positive population, 65 % (32/49) of the patients had evidence of venous invasion. Furthermore, 76 % (32/42) of patients with lymph node metastasis were *XAF1F* positive ($p = 0.0101$). To investigate the relationship between this metastasis and lymphatic invasion, we further analyzed the frequency of invasion in *XAF1F*-positive patients with lymph node metastasis. Although this splice variant was not correlated with lymphatic invasion in 79 patients with CTCs, 27 of 32 patients with metastasis (N1, 2, 3) had lymphatic invasion (84 %), whereas 82 % of patients without metastasis (N0) had no lymphatic invasion (14/17, $p = 7.528 \times 10^{-6}$ in Fisher's exact test). This result indicates that the lymph node metastasis associated with *XAF1F*-expressing CTCs accompanies lymphatic invasion. These CTCs may therefore easily metastasize to a lymph node rather than a lymphatic vessel.

Discussion

Alternative splicing allows a single gene to generate multiple mRNAs that can be translated into diverse proteins

Table 2 Expression of XAF1F and XAF1C in clinicopathological characteristics of circulating tumor cell (CTC)-containing patients

	XAF1F			*XAF1C*			*XAF1F/C*		
	Positive ($n = 49$)	Negative ($n = 30$)	p value	Positive ($n = 36$)	Negative ($n = 43$)	p value	Positive ($n = 26$)	Negative ($n = 53$)	p value
Gender			NS			NS			NS
Male	33	20		25	28		16	37	
Female	16	10		11	15		10	16	
Depth of tumor invasion			0.0368			NS			NS
≤MP[a] (T2)	20	20		16	24		11	29	
≥SS[b] (T3)	29	10		20	19		15	24	
Lymph node metastasis			0.0101			NS			NS
N0	17	20		17	20		11	26	
N1, 2, 3	32	10		19	23		15	27	
Peritoneal cytology			NS			NS			NS
CY0	7	1		2	6		2	6	
CY1	42	29		34	37		24	47	
Stage			NS			NS			NS
I, II	27	23		25	26		17	33	
III, IV	22	7		11	17		9	20	
Histological typing			NS			NS			NS
Differentiated	19	15		17	17		10	24	
Undifferentiated	30	15		19	26		16	29	
Lymphatic invasion			NS			NS			NS
ly0	19	17		17	19		13	23	
ly1, 2, 3	30	13		19	24		13	30	
Venous invasion			0.0011			NS			NS
v0	17	22		18	21		10	29	
v1, 2, 3	32	8		18	22		16	24	
Recurrence			NS			NS			NS
Yes	3	0		1	2		1	2	
No	46	30		35	41		25	51	

Test used: Fisher's exact test

NS not significant

[a] Muscularis propria

[b] Subserosa

[48]. Many transcripts have been predicted by in silico approaches and registered in public databases (e.g., Ensembl, http://www.ensembl.org) as candidate splice variants [49, 50]. Recently, Furuta et al. [51, 52] and our research group independently found that aberrant alternative splicing in cancer cells results in the insertion of intronic regions as extended exons, which results in the generation of new splice variants. Thus, it is important to explore the intronic regions of target genes to find novel splice variants, and here, we investigated the exons and introns of *XAF1* simultaneously.

In agreement with previous reports [2, 12], *XAF1* was downregulated in more than half the cell lines tested. However, the *XAF1F* transcript harboring a PTC was not often coexpressed with other *XAF1* transcripts. Comparative analysis of metastatic models obtained by xenografting (MKN45P vs. MKN45 and KP-3L vs. KP-3) revealed that the *XAF1F* and NMD target genes were upregulated in MKN45P and KP-3L cells. These data suggest that the NMD pathway in *XAF1F*-expressing cells with metastatic potential is suppressed relative to the parent cells. Recent studies have shown that tumor growth and metastasis are facilitated by NMD inhibition [53, 54]. The suppression of the NMD pathway in MKN45P and KP-3L cells may therefore be associated with cancer metastasis.

We found that the *XAF1F* transcript harboring PTC was upregulated in NMD-suppressed cancer cells and presumably subjected to NMD. To elucidate the degradation of the

XAF1F transcript through the NMD pathway, an NMD inhibition assay was performed. The NMD factor *UPF1* and NMD target genes (Fig. 3a) were significantly upregulated in KP-3L cells, which raises the possibility that NMD inhibition in *XAF1F*-expressed cells is regulated by other NMD factors. Therefore, we used caffeine as an NMD inhibitor [37] rather than depletion of *UPF1* by RNAi [16]. In cancer cells treated with only actD, which blocks transcription, *XAF1F* expression was decreased, indicating that this transcript is especially unstable in cells with active NMD. In contrast, *XAF1F* accumulated in cells in which NMD was inhibited with caffeine. These results suggest that the PTC-harboring *XAF1F* is degraded through the NMD pathway. Therefore, we concluded that expression analysis of this splice variant is valuable to evaluate NMD inhibition in cancer cells.

Splice variants of *XAF1* have been found to be significantly upregulated in the peripheral blood of gastric cancer patients. Furthermore, survivin, which is considered to be expressed in CTCs, is also detected in many patients. Therefore, *XAF1* variants are likely to be derived from CTCs. However, use of the qRT-PCR assay and PAXgene cannot eliminate the influence of circulating cell-free RNA [55] (including mRNA in microvesicles or exosomes [56, 57]) and lymphocytes or other nucleated cells because of the stabilization of whole RNA in the peripheral blood. Further studies should thus investigate the expression of *XAF1* variants in CTCs isolated using immunomagnetic separation systems (such as CellSearch). However, Chi et al. reported that *XAF1* transcripts are significantly downregulated in gastric and colorectal tumors [2, 12]. If the upregulated *XAF1* transcripts that we observed are derived from CTCs, then the expression levels of these transcripts would thus be inconsistent between the tumor tissue and CTCs. Several reports described such a difference in the gene expression profiles of primary tumors and CTCs [58, 59]. This discrepancy should be also examined using isolated CTCs in further studies.

We further attempted to discriminate survivin-positive patients using the cutoff value calculated from the ROC curve to identify the population who had CTCs. Among the patients, 82 % (79/96) were categorized as survivin-expressing CTC-positive patients, which was similar to the discriminative performance in a previous study using RT-PCR ELISA [35]. Furthermore, the *XAF1F/C*-positive population accounted for approximately half the CTC-positive patients and showed significant expression of the *ATF3* transcript. These results suggest that the NMD pathway is often suppressed in peripheral blood containing survivin-expressing CTCs derived from gastric cancer. Recently, several research groups have reported that heterogeneity may lead to differences in protein expression or cellular adhesion in CTCs [60–62]. The NMD-suppressed population identified in this study may also contribute to the heterogeneity of CTCs.

XAF1 in cancer cells acts as a tumor suppressor because of its pro-apoptotic function (Fig. 6) [13]. *XAF1* expression in various cancer cell types was found to be transcriptionally inactivated by the methylation of CpG sites in the promoter region [9, 10]. Heat shock factor (HSF)1 and p53 can also negatively regulate the *XAF1* gene via the binding of these binding elements [63, 64]. Several studies have demonstrated that *XAF1* is upregulated by interferon (IFN), resulting in the sensitization of cells to apoptosis [65–69]. To our knowledge, this study is the first to show that *XAF1F* is generated by aberrant pre-mRNA processing through NMD inhibition, which is often induced by cellular stress in the tumor microenvironment [17–19]. The *XAF1F*-expressing cells with inhibition of NMD may be stressed by external stimuli or have an amplified cellular stress response. Our qRT-PCR assay revealed that the NMD pathway tends to be inhibited in some CTCs from gastric cancer. Several studies have demonstrated that CTCs exposed to blood flow undergo physiological shear stress, leading to a change in the gene expression pattern [70, 71]. These findings suggest that *XAF1F*-expressing CTCs with inhibition of NMD may be strongly stressed by the external environment in comparison with the *XAF1F*-negative population or that they may be highly sensitive to stress.

Recent studies detected CTCs from gastric or hepatocellular cancer in patients with vascular invasion [72, 73], whereas CTCs derived from head and neck cancer were associated with lymph node metastasis [74, 75], indicating that these characteristics depend on the primary tumor. In our study, the mRNA expression level of *XAF1F* in CTCs was significantly correlated with venous invasion, lymph node metastasis, and tumor invasion that reached the SS. Additionally, the lymph node metastasis associated with *XAF1F*-expressing CTCs accompanied lymphatic invasion. Metastatic cells in which the EMT has occurred have been shown to penetrate local tissue and blood or lymphatic vessels [76]. These findings raise the possibility that *XAF1F*-positive CTCs in gastric cancer have the characteristics of EMT. In several cancer cell types, the EMT is closely related with RNA splicing [28] or NMD inhibition that can generate aberrant transcripts [29]. Therefore, CTCs expressing splice variants via NMD suppression may have been phenotypically converted by the EMT. At the minimum, these findings suggest that expression of both *XAF1F* and survivin in the peripheral blood of gastric cancer patients is a predictor of venous invasion, lymph node metastasis, and depth of tumor invasion.

A significant correlation was found between *XAF1F* in CTCs and the depth of tumor invasion/lymph node metastasis, whereas *XAF1F* expression tended to be associated with the stage of gastric cancer ($p = 0.05985$ in

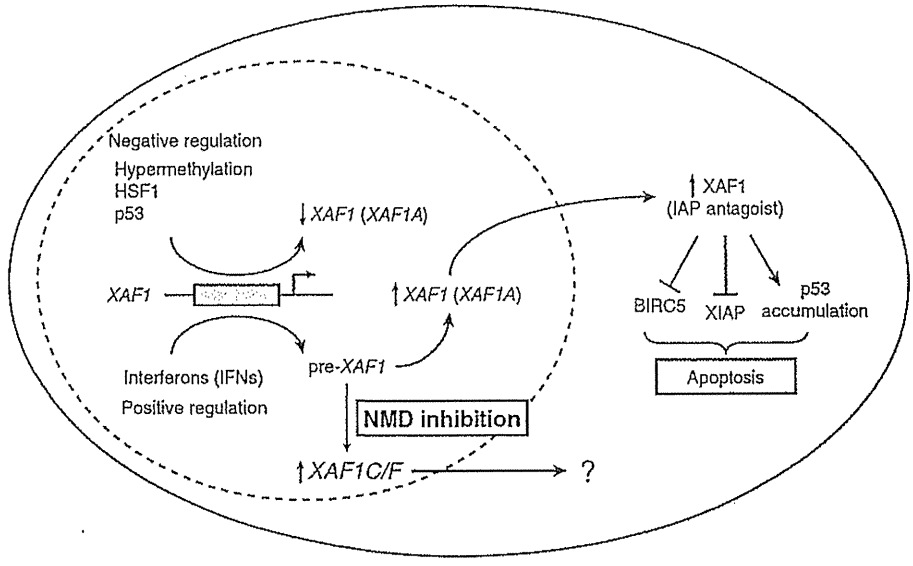

Fig. 6 Key roles of XAF1 in cancer cells. The transcription of the *XAF1* gene is under the control of negative and positive regulatory elements. NMD inhibition promotes accumulation of *XAF1F*. *Gray arrows* indicate the upregulation or downregulation of the *XAF1* transcripts. HSF and XIAP represent heat shock factor 1 and XIAP, respectively

Fisher's exact test). In stage I and II, 67 % (2/3) and 90 % (9/10) of patients with lymph node metastasis were categorized as *XAF1F* positive, respectively. These results suggest that *XAF1F* expression in CTCs strongly reflects lymph node metastasis in stage I and II, leading to a weak association between *XAF1F* expression and tumor stage. Additionally, *XAF1F* expression in CTCs was not associated with recurrence, although CTCs are useful as a prognostic factor [36, 44–47]. In further studies, this discrepancy should be also examined using long-term follow-up data of CTCs isolated from patients to clarify the origin of the *XAF1* variant.

In conclusion, the present study identified a novel splice variant of *XAF1* in gastric, pancreatic, colorectal, and breast cancer cells. This variant was regulated through the NMD pathway and accumulated in NMD-suppressed metastatic cancer cells. To our knowledge, this is the first study to clearly detect *XAF1* variants in peripheral blood containing CTCs derived from gastric cancer. The expression of these variants was significantly higher than that in healthy volunteers. Furthermore, in part of the CTC-positive population, the NMD pathway was suppressed. These findings suggest that *XAF1* variants accumulate by NMD inhibition in the peripheral blood of gastric cancer patients and may indicate heterogeneity of CTCs.

Acknowledgments This research was supported by a Grant-in-Cooperation of the Regional Innovation Cluster Program 2010 and Japan Society for the Promotion of Science KAKENHI 23701092 and 25710013. The authors thank Yuko Watanabe, Kaori Kanto, and Tomomi Ide for their technical assistance, Keita Mori for statistical advice, and Dr. Takashi Sugino for comments on the clinicopathological data.

Conflict of interest The authors have no conflict of interest.

References

1. Liston P, Fong WG, Kelly NL, et al. Identification of XAF1 as an antagonist of XIAP anti-caspase activity. Nat Cell Biol. 2001;3(2):128–33.
2. Byun DS, Cho K, Ryu BK, et al. Hypermethylation of XIAP-associated factor 1, a putative tumor suppressor gene from the 17p13.2 locus, in human gastric adenocarcinomas. Cancer Res. 2003;63(21):7068–75.
3. Arora V, Cheung HH, Plenchette S, et al. Degradation of survivin by the X-linked inhibitor of apoptosis (XIAP)-XAF1 complex. J Biol Chem. 2007;282(36):26202–9.
4. Tu SP, Liston P, Cui JT, et al. Restoration of XAF1 expression induces apoptosis and inhibits tumor growth in gastric cancer. Int J Cancer. 2009;125(3):688–97.
5. Huang J, Yao WY, Zhu Q, et al. XAF1 as a prognostic biomarker and therapeutic target in pancreatic cancer. Cancer Sci. 2010;101(2):559–67.
6. Sun PH, Zhu LM, Qiao MM, et al. The XAF1 tumor suppressor induces autophagic cell death via upregulation of Beclin-1 and inhibition of Akt pathway. Cancer Lett. 2011;310(2):170–80.
7. Zou B, Chim CS, Pang R, et al. XIAP-associated factor 1 (XAF1), a novel target of p53, enhances p53-mediated apoptosis via post-translational modification. Mol Carcinog. 2012;51(5):422–32.
8. Fong WG, Liston P, Rajcan-Separovic E, et al. Expression and genetic analysis of XIAP-associated factor 1 (XAF1) in cancer cell lines. Genomics. 2000;70(1):113–22.
9. Zou B, Chim CS, Zeng H, et al. Correlation between the single-site CpG methylation and expression silencing of the XAF1 gene in human gastric and colon cancers. Gastroenterology. 2006;131(6):1835–43.
10. Lee MG, Huh JS, Chung SK, et al. Promoter CpG hypermethylation and downregulation of XAF1 expression in human urogenital malignancies: implication for attenuated p53 response to apoptotic stresses. Oncogene. 2006;25(42):5807–22.
11. Yin W, Cheepala S, Clifford JL. Identification of a novel splice variant of X-linked inhibitor of apoptosis-associated factor 1. Biochem Biophys Res Commun. 2006;339(4):1148–54.
12. Chung SK, Lee MG, Ryu BK, et al. Frequent alteration of XAF1 in human colorectal cancers: implication for tumor cell resistance to apoptotic stresses. Gastroenterology. 2007;132(7):2459–77.

13. Plenchette S, Cheung HH, Fong WG, et al. The role of XAF1 in cancer. Curr Opin Invest Drugs. 2007;8(6):469–76.
14. Fang X, Liu Z, Fan Y, et al. Switch to full-length of XAF1 mRNA expression in prostate cancer cells by the DNA methylation inhibitor. Int J Cancer. 2006;118(10):2485–9.
15. Maquat LE. Nonsense-mediated mRNA decay. Curr Biol. 2002;12(6):R196–7.
16. Mendell JT, Sharifi NA, Meyers JL, et al. Nonsense surveillance regulates expression of diverse classes of mammalian transcripts and mutes genomic noise. Nat Genet. 2004;36(10):1073–8.
17. Gardner LB. Nonsense-mediated RNA decay regulation by cellular stress: implications for tumorigenesis. Mol Cancer Res. 2010;8(3):295–308.
18. Gardner LB. Hypoxic inhibition of nonsense-mediated RNA decay regulates gene expression and the integrated stress response. Mol Cell Biol. 2008;28(11):3729–41.
19. Wang D, Zavadil J, Martin L, et al. Inhibition of nonsense-mediated RNA decay by the tumor microenvironment promotes tumorigenesis. Mol Cell Biol. 2011;31(17):3670–80.
20. Tani H, Torimura M, Akimitsu N. The RNA degradation pathway regulates the function of GAS5 a non-coding RNA in mammalian cells. PLoS One. 2013;8(1):e55684.
21. Wang S, Zheng G, Cheng B, et al. Circulating tumor cells (CTCs) detected by RT-PCR and its prognostic role in gastric cancer: a meta-analysis of published literature. PLoS One. 2014;9(6):e99259.
22. Powell AA, Talasaz AH, Zhang H, et al. Single cell profiling of circulating tumor cells: transcriptional heterogeneity and diversity from breast cancer cell lines. PLoS One. 2012;7(5):e33788.
23. Neuert G, Munsky B, Tan RZ, et al. Systematic identification of signal-activated stochastic gene regulation. Science. 2013;339(6119):584–7.
24. Zhang ZY, Ge HY. Micrometastasis in gastric cancer. Cancer Lett. 2013;336(1):34–45.
25. Savagner P, Valles AM, Jouanneau J, et al. Alternative splicing in fibroblast growth factor receptor 2 is associated with induced epithelial-mesenchymal transition in rat bladder carcinoma cells. Mol Biol Cell. 1994;5(8):851–62.
26. Pino MS, Balsamo M, Di Modugno F, et al. Human Mena+11a isoform serves as a marker of epithelial phenotype and sensitivity to epidermal growth factor receptor inhibition in human pancreatic cancer cell lines. Clin Cancer Res. 2008;14(15):4943–50.
27. Warzecha CC, Sato TK, Nabet B, et al. ESRP1 and ESRP2 are epithelial cell-type-specific regulators of FGFR2 splicing. Mol Cell. 2009;33(5):591–601.
28. Shapiro IM, Cheng AW, Flytzanis NC, et al. An EMT-driven alternative splicing program occurs in human breast cancer and modulates cellular phenotype. PLoS Genet. 2011;7(8):e1002218.
29. Valacca C, Bonomi S, Buratti E, et al. Sam68 regulates EMT through alternative splicing-activated nonsense-mediated mRNA decay of the SF2/ASF proto-oncogene. J Cell Biol. 2010;191(1):87–99.
30. Fujita Y, Terashima M, Hoshino Y, et al. Detection of cancer cells disseminated in bone marrow using real-time quantitative RT-PCR of CEA, CK19, and CK20 mRNA in patients with gastric cancer. Gastric Cancer. 2006;9(4):308–14.
31. Huang P, Wang J, Guo Y, et al. Molecular detection of disseminated tumor cells in the peripheral blood in patients with gastrointestinal cancer. J Cancer Res Clin Oncol. 2003;129(3):192–8.
32. Ishigami S, Sakamoto A, Uenosono Y, et al. Carcinoembryonic antigen messenger RNA expression in blood can predict relapse in gastric cancer. J Surg Res. 2008;148(2):205–9.
33. Helo P, Cronin AM, Danila DC, et al. Circulating prostate tumor cells detected by reverse transcription-PCR in men with localized or castration-refractory prostate cancer: concordance with Cell Search assay and association with bone metastases and with survival. Clin Chem. 2009;55(4):765–73.
34. Danila DC, Anand A, Schultz N, et al. Analytic and clinical validation of a prostate cancer-enhanced messenger RNA detection assay in whole blood as a prognostic biomarker for survival. Eur Urol 2014;65(6):1191–7
35. Cao W, Yang W, Li H, et al. Using detection of survivin-expressing circulating tumor cells in peripheral blood to predict tumor recurrence following curative resection of gastric cancer. J Surg Oncol. 2011;103(2):110–5.
36. Cao M, Yie SM, Wu SM, et al. Detection of survivin-expressing circulating cancer cells in the peripheral blood of patients with esophageal squamous cell carcinoma and its clinical significance. Clin Exp Metastasis. 2009;26(7):751–8.
37. Ivanov I, Lo KC, Hawthorn L, et al. Identifying candidate colon cancer tumor suppressor genes using inhibition of nonsense-mediated mRNA decay in colon cancer cells. Oncogene. 2007;26(20):2873–84.
38. Robin X, Turck N, Hainard A, et al. pROC: an open-source package for R and S+ to analyze and compare ROC curves. BMC Bioinform. 2011;12:77.
39. Xia J, Broadhurst DI, Wilson M, et al. Translational biomarker discovery in clinical metabolomics: an introductory tutorial. Metabolomics. 2013;9(2):280–99.
40. Huang L, Lou CH, Chan W, et al. RNA homeostasis governed by cell type-specific and branched feedback loops acting on NMD. Mol Cell. 2011;43(6):950–61.
41. Chan WK, Huang L, Gudikote JP, et al. An alternative branch of the nonsense-mediated decay pathway. EMBO J. 2007;26(7):1820–30.
42. Schroeder A, Mueller O, Stocker S, et al. The RIN: an RNA integrity number for assigning integrity values to RNA measurements. BMC Mol Biol. 2006;7:3.
43. Bruning O, Rodenburg W, Radonic T, et al. RNA isolation for transcriptomics of human and mouse small skin biopsies. BMC Res Notes. 2011;4:438.
44. Yie SM, Lou B, Ye SR, et al. Detection of survivin-expressing circulating cancer cells (CCCs) in peripheral blood of patients with gastric and colorectal cancer reveals high risks of relapse. Ann Surg Oncol. 2008;15(11):3073–82.
45. Bertazza L, Mocellin S, Marchet A, et al. Survivin gene levels in the peripheral blood of patients with gastric cancer independently predict survival. J Transl Med. 2009;7:111.
46. Hoffmann AC, Warnecke-Eberz U, Luebke T, et al. Survivin mRNA in peripheral blood is frequently detected and significantly decreased following resection of gastrointestinal cancers. J Surg Oncol. 2007;95(1):51–4.
47. Terashima M, Yamakawa Y, Hatakeyama K, et al. Survivin expression in peripheral blood as a prognostic marker in patients with gastric cancer. J Clin Oncol 2014;32(suppl 15).
48. Black DL. Mechanisms of alternative pre-messenger RNA splicing. Annu Rev Biochem. 2003;72:291–336.
49. Birney E, Andrews D, Bevan P, et al. Ensembl 2004. Nucleic Acids Res 2004;32(database issue):D468–D470.
50. Birney E, Andrews TD, Bevan P, et al. An overview of Ensembl. Genome Res. 2004;14(5):925–8.
51. Furuta K, Arao T, Sakai K, et al. Integrated analysis of whole genome exon array and array-comparative genomic hybridization in gastric and colorectal cancer cells. Cancer Sci. 2012;103(2):221–7.
52. Hatakeyama K, Ohshima K, Fukuda Y, et al. Identification of a novel protein isoform derived from cancer-related splicing variants using combined analysis of transcriptome and proteome. Proteomics. 2011;11(11):2275–82.
53. Pastor F, Kolonias D, Giangrande PH, et al. Induction of tumour immunity by targeted inhibition of nonsense-mediated mRNA decay. Nature (Lond). 2010;465(7295):227–30.

54. Bonomi S, di Matteo A, Buratti E, et al. HnRNP A1 controls a splicing regulatory circuit promoting mesenchymal-to-epithelial transition. Nucleic Acids Res. 2013;41(18):8665–79.
55. Garcia-Olmo DC, Ruiz-Piqueras R, Garcia-Olmo D. Circulating nucleic acids in plasma and serum (CNAPS) and its relation to stem cells and cancer metastasis: state of the issue. Histol Histopathol. 2004;19(2):575–83.
56. Valadi H, Ekstrom K, Bossios A, et al. Exosome-mediated transfer of mRNAs and microRNAs is a novel mechanism of genetic exchange between cells. Nat Cell Biol. 2007;9(6):654–9.
57. Ohshima K, Inoue K, Fujiwara A, et al. Let-7 microRNA family is selectively secreted into the extracellular environment via exosomes in a metastatic gastric cancer cell line. PLoS One. 2010;5(10):e13247.
58. Meng S, Tripathy D, Shete S, et al. HER-2 gene amplification can be acquired as breast cancer progresses. Proc Natl Acad Sci USA. 2004;101(25):9393–8.
59. Gradilone A, Petracca A, Nicolazzo C, et al. Prognostic significance of survivin-expressing circulating tumour cells in T1G3 bladder cancer. BJU Int. 2010;106(5):710–5.
60. Krebs MG, Hou JM, Sloane R, et al. Analysis of circulating tumor cells in patients with non-small cell lung cancer using epithelial marker-dependent and -independent approaches. J Thorac Oncol. 2012;7(2):306–15.
61. Zhao L, Li P, Li F, et al. The prognostic value of circulating tumor cells lacking cytokeratins in metastatic breast cancer patients. J Cancer Res Ther. 2013;9(1):29–37.
62. Hosokawa M, Kenmotsu H, Koh Y, et al. Size-based isolation of circulating tumor cells in lung cancer patients using a microcavity array system. PLoS One. 2013;8(6):e67466.
63. Wang J, He H, Yu L, et al. HSF1 down-regulates XAF1 through transcriptional regulation. J Biol Chem. 2006;281(5):2451–9.
64. Zhang W, Guo Z, Jiang B, et al. Identification of a functional p53 responsive element within the promoter of XAF1 gene in gastrointestinal cancer cells. Int J Oncol. 2010;36(4):1031–7.
65. Leaman DW, Chawla-Sarkar M, Vyas K, et al. Identification of X-linked inhibitor of apoptosis-associated factor-1 as an interferon-stimulated gene that augments TRAIL Apo2L-induced apoptosis. J Biol Chem. 2002;277(32):28504–11.
66. Chawla-Sarkar M, Lindner DJ, Liu YF, et al. Apoptosis and interferons: role of interferon-stimulated genes as mediators of apoptosis. Apoptosis. 2003;8(3):237–49.
67. Wang J, Peng Y, Sun YW, et al. All-trans retinoic acid induces XAF1 expression through an interferon regulatory factor-1 element in colon cancer. Gastroenterology. 2006;130(3):747–58.
68. Micali OC, Cheung HH, Plenchette S, et al. Silencing of the XAF1 gene by promoter hypermethylation in cancer cells and reactivation to TRAIL-sensitization by IFN-beta. BMC Cancer. 2007;7:52.
69. Reu FJ, Bae SI, Cherkassky L, et al. Overcoming resistance to interferon-induced apoptosis of renal carcinoma and melanoma cells by DNA demethylation. J Clin Oncol. 2006;24(23):3771–9.
70. Mitchell MJ, King MR. Computational and experimental models of cancer cell response to fluid shear stress. Front Oncol. 2013;3:44.
71. Gakhar G, Navarro VN, Jurish M, et al. Circulating tumor cells from prostate cancer patients interact with E-selectin under physiologic blood flow. PLoS One. 2013;8(12):e85143.
72. Kutun S, Celik A, Cem Kockar M, et al. Expression of CK-19 and CEA mRNA in peripheral blood of gastric cancer patients. Exp Oncol. 2010;32(4):263–8.
73. Schulze K, Gasch C, Staufer K, et al. Presence of EpCAM-positive circulating tumor cells as biomarker for systemic disease strongly correlates to survival in patients with hepatocellular carcinoma. Int J Cancer. 2013;133(9):2165–71.
74. Partridge M, Brakenhoff R, Phillips E, et al. Detection of rare disseminated tumor cells identifies head and neck cancer patients at risk of treatment failure. Clin Cancer Res. 2003;9(14):5287–94.
75. Hristozova T, Konschak R, Stromberger C, et al. The presence of circulating tumor cells (CTCs) correlates with lymph node metastasis in nonresectable squamous cell carcinoma of the head and neck region (SCCHN). Ann Oncol. 2011;22(8):1878–85.
76. Tsuji T, Ibaragi S, Hu GF. Epithelial-mesenchymal transition and cell cooperativity in metastasis. Cancer Res. 2009;69(18):7135–9.

FOCUS

胃癌に対するロボット手術の現況

寺島　雅典　　徳永　正則　　谷澤　　豊　　坂東　悦郎
川村　泰一　　幕内　梨恵　　三木友一朗　　絹笠　祐介
上坂　克彦

臨　床　外　科
第69巻　第12号 別刷
2014年11月20日　発行

医学書院

FOCUS

胃癌に対するロボット手術の現況

静岡県立静岡がんセンター胃外科[1]　同 消化器外科[2]

寺島雅典[1]　徳永正則[1]　谷澤　豊[1]　坂東悦郎[1]　川村泰一[1]
幕内梨恵[1]　三木友一朗[1]　絹笠祐介[2]　上坂克彦[2]

はじめに

手術支援ロボットとして広く普及しているda Vinci Surgical Systemは1988年に開発され，高解像度の3D画像と，7自由度をもつEndoWrsitを搭載することにより，内視鏡下でも可動制限のない自然な操作感で手術を行うことが可能である．2014年4月現在，全世界で約3,000台が稼働しており，わが国でも174台が納入され，米国に次いで世界第2位のロボット手術大国となっている．その大きな推進力となったのは，2012年4月に承認された前立腺全摘除術に対する保険適用であり，これ以降，多くの施設で泌尿器科を中心にロボット支援手術が導入されるようになった．

わが国におけるロボット胃切除の現況

2009年にda Vinci Surgical Systemがわが国で薬事承認を受け，胃切除に関しては藤田保健衛生大学で第1例目の手術が行われた．それ以降，わずかずつではあるが順調に症例数が増加しており，特に機器の導入が加速度的に増加した2012年以降，胃切除の月次症例数も増加傾向にある．これまで約500例に対してロボット支援下の胃切除術が行われている（**図1**）．

現在，35施設でロボット支援下胃切除術が導入されている．当科でもこれまで101例のロボット支援下胃切除を施行したが，わが国で50例以上の手術経験がある施設は藤田保健衛生大学と当院だけであり，20例以上の施設としても5施設のみで，ほとんどの施設では10例以下の臨床経験に留まっている．これはいまだ導入初期の施設が多いことと，保険適用が得られていないため手術費用負担が大きいことに起因しているものと思われる．

ロボット胃切除の研究報告

胃切除に関しては，2003年にHashizumeら[1)]が報告して以来，日本，イタリア，韓国を中心としてロボット支援胃切除術が普及してきた．これまで報告された論文の一覧を**表1**に示したが，ほとんどの論文がいわゆる臨床経験をまとめたケースシリーズか，後ろ向きのケースコントロール研究であり，極めてエビデンスレベルの低い報告ばかりである．当科でロボット手術を開始した2011年の時点では，前向きの研究は一つも行われていなかったため，よりエビデンスレベルの高い研究を行うことを目的として，ロボット支援胃切除の安全性を評価する前向きの前期臨床第Ⅱ相試験を実施した．その結果はすでに報告されているが[2)]，対象はcStageⅠA症例とし，腹腔内感染性合併症の発生割合を主要評価項目として，23例（解析対象は初期5例を除く18例）で評価した．その結果，腹腔内感染性合併症の発生を1例も認めず，試験結果はポジティブと判定された．現在，cStageⅠBまで適応を拡大し，全摘や噴切も含めた後期臨床第Ⅱ相試験

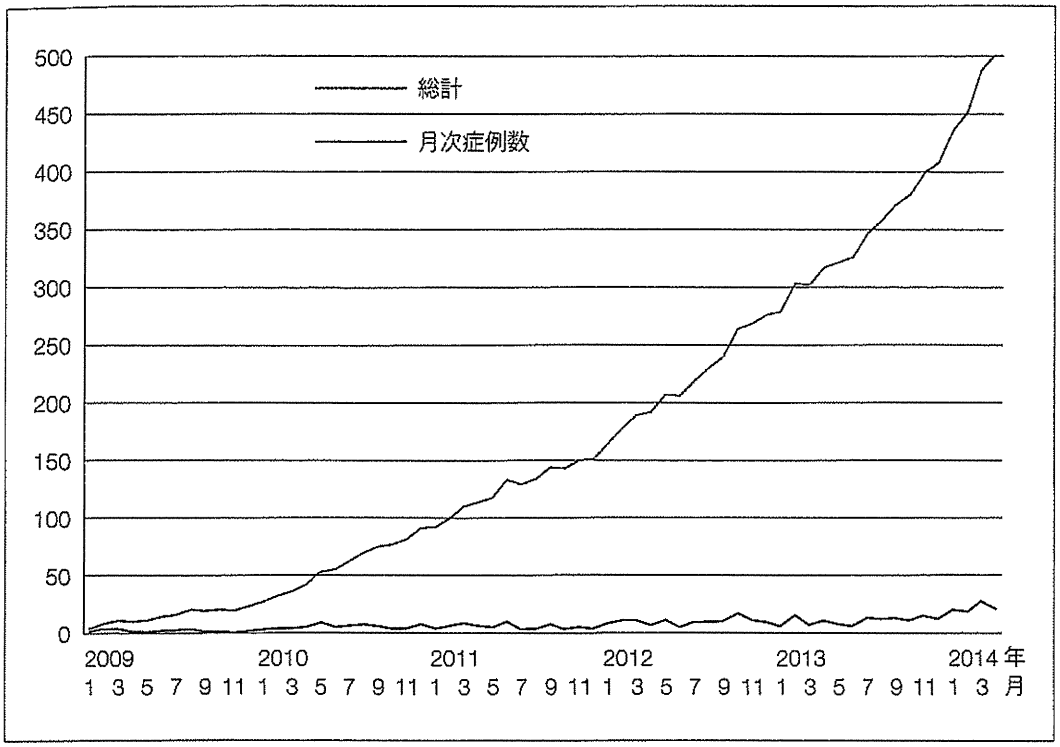

図1　わが国におけるロボット胃切除術症例数の推移

を実施中である．予定集積症例は100例としている．

開腹手術や腹腔鏡下手術との比較に関しても，ほとんどの研究が後ろ向きのケースコントロール研究である．これらの研究では症例数も一部の報告を除いては100例未満で，背景因子にも大きなバイアスが存在し，あまり有益な情報は提示されていない．しかしながら，最近これらの報告をまとめて解析するメタ解析の論文が相次いで報告されている[3~9]．その一覧を表2に示したが，無作為化比較試験の報告が一つもない状況で，メタ解析を施行しても明確な結論を得ることは困難と思われる．また，多くの報告ではロボット手術症例が数十例のみで，韓国のYonsei大学とAjou大学からの報告だけが100例を超えている．したがって，多くの報告を解析対象に加えたとしても，解析結果はこれらの症例数の多い結果に大きく左右されてしまうため，あまりメタ解析をする意味がないのも事実である．ただし，開腹手術との比較ではロボット手術で手術時間が長く，出血量が少なく，在院日数が短いこと，腹腔鏡下手術との比較ではロボット手術で手術時間が長く，出血量が少なく，肛門側マージンが長いことが示されている．そのほかの因子として，リンパ節郭清個数，術後合併症の発生頻度なども解析されているが，いずれも差が認められなかった．多くの施設ではロボット手術導入初期の成績であり，すでに習熟した腹腔鏡下手術との比較であることを考慮すると，ロボット手術は比較的安全，確実な方法であることが示唆されているものと思われる．

ラーニングカーブ

ロボット手術の一つの大きな利点として，腹腔鏡下手術に比較してラーニングカーブが短いことが挙げられる．ロボット支援胃切除についても，ラーニングカーブに関していくつか報告がなされている．Kangら[10]はKorea大学におけるロボット胃切除100例の経験から，初期20例とそれ以後の80例とに分類したところ，手術時間と在院日数に有意な差を認め，20例以上経験すれば良好な成績が得られると報告している．また，Parkら[11]は韓国の3施設で，腹腔鏡下胃切除の十分な経験を有する外科医におけるロボット胃切除のラーニングカーブについて検討し，安定した手術時間に到達するには平均で8.2例が必要であるとしている．腹腔鏡下胃切除術においては安定した手術時間に到達するには通常50例以上が必要とされるため[12]，腹腔鏡下手術の十分な経験を有する外科医にとっては，ロボット手術のラーニングカーブは極めて